Juvenile hormone-induced histone deacetylase 3 suppresses apoptosis to maintain larval midgut in the yellow fever mosquito

Sharath Chandra Gaddelapati[a], Najla M. Albishi[a], Ramesh Kumar Dhandapani[a], and Subba Reddy Palli[a,1]

[a]Department of Entomology, University of Kentucky, Lexington, KY 40546

Edited by Lynn Riddiford, University of Washington, Friday Harbor, WA; received October 14, 2021; accepted January 30, 2022

The yellow fever mosquito, *Aedes aegypti*, is distributed worldwide and transmits viruses that cause many diseases, including dengue, yellow fever, chikungunya, and zika. Epigenetic modifications such as acetylation of histones regulated by histone acetyltransferases (HATs) and histone deacetylases (HDACs) control insect development. We recently reported that the Creb-binding protein (a HAT) regulates the metamorphosis of *A. aegypti*. However, the function of HDACs in *A. aegypti* is not known. In this study, we identified 10 genes coding for HDACs in *A. aegypti* and determined their function in larval development using RNA interference (RNAi). Knockdown of each HDAC has a distinct effect on the growth, development, and metamorphosis of *A. aegypti*. Knockdown of HDAC3 severely affected the larval survival, indicating its indispensable role in larval development. HDAC3 is highly expressed during the larval stages, and its messenger RNA (mRNA) levels correlate with the juvenile hormone (JH) titers. JH induces the expression of *HDAC3* through its receptor, methoprene-tolerant (Met). Knockdown of *HDAC3* resulted in increased expression of proapoptotic genes involved in apoptosis of larval midgut cells. This consequently decreased midgut size and led to larval death. HDAC3 deacetylates histone H4 localized at the promoters of proapoptotic genes and suppresses their expression. In addition, a corepressor, SMRTER, is required for HDAC3-mediated suppression of proapoptotic genes. Interestingly, ecdysone attenuates HDAC3-mediated repression of proapoptotic genes. These data demonstrate that JH-induced HDAC3 is a key player in JH suppression of precocious larval cell death and metamorphosis in *A. aegypti*.

epigenetics | histone deacetylase | *Aedes aegypti* | apoptosis | midgut-remodeling

Arthropod-borne arboviruses are a major threat to human health. The yellow fever mosquito, *Aedes aegypti*, is a major vector of human arboviruses that cause dengue, Zika, yellow fever, chikungunya, and other diseases. A widespread epidemic of zika across Central and South America and the Caribbean has been linked to fetal brain abnormalities (1). Dengue is the most-common human arboviral disease infecting millions of people each year. Over the last decade, chikungunya emerged as one of the major epidemics in Asia, Europe, and America. Adult female mosquitoes transmit the above arboviruses during blood-feeding on hosts. Therefore, blocking the transition from the immature to an adult stage could be a useful strategy to prevent the spread of mosquito-borne diseases.

Epigenetic modifications regulate genome expression by turning on or off a network of genes resulting in different phenotypes from a common genotype (2). Aberrations in epigenetic regulation can affect growth and development and cause diseases such as cancer. The main classes of epigenetic modifiers are chromatin remodelers (affect DNA–histone interactions) and histone modifiers (affect histone posttranslational modifications) that alter chromatin organization. Acetylation is one of the major histone modifications carried by histone acetyltransferases (HATs) that neutralize the positive charge of histones, thereby relaxing chromatin structure. This provides target gene promoter access to the transcription factors and RNA polymerase complexes to activate gene expression. In contrast, histone deacetylases (HDACs) remove acetyl groups from the lysine residues in the histone tails, resulting in chromatin compaction and repression of the target gene expression. Histone acetylation regulates many developmental processes in insects. Histone acetylation by Creb-binding protein (CBP) initiates dendrite pruning in *Drosophila melanogaster* (3). The inhibition of HDAC activity alters caste specification in honeybees (4). HDACs also regulate mandibles and wing sizes in the broad-horned flour beetle, *Gnatocerus cornutus* (5). Equilibrium between CBP-mediated histone acetylation and HDAC-mediated histone deacetylation in the brain regulates caste-specific foraging and scouting behaviors in the ant, *Camponotus floridanus* (6). HATs and HDACs antagonistically regulate nuclear receptor expression and activity during insect metamorphosis (7, 8).

Previously, we showed that CBP acetylates histones and regulates the transcription of genes involved in JH and ecdysone signaling in *A. aegypti* and *Tribolium castaneum* (9–11). In contrast, the inhibition of HDAC activity using Trichostatin A inhibitor or knockdown of genes coding for HDACs affected the metamorphosis of *T. castaneum* (11–14). Specifically, *HDAC1* knockdown increased expression of JH response genes,

Significance

Juvenile hormone (JH), a sesquiterpenoid, regulates many aspects of insect development, including maintenance of the larval stage by preventing metamorphosis. In contrast, ecdysteroids promote metamorphosis by inducing the *E93* transcription factor, which triggers apoptosis of larval cells and remodeling of the larval midgut. We discovered that JH suppresses precocious larval midgut-remodeling by inducing an epigenetic modifier, histone deacetylase 3 (*HDAC3*). JH-induced *HDAC3* deacetylates the histone H4 localized at the promoters of proapoptotic genes, resulting in the suppression of these genes. This eventually prevents programmed cell death of midgut cells and midgut-remodeling during larval stages. These studies identified a previously unknown mechanism of JH action in blocking premature remodeling of the midgut during larval feeding stages.

Author contributions: S.C.G. and S.R.P. designed research; S.C.G., N.M.A., and R.K.D. performed research; S.C.G., N.M.A., and R.K.D. analyzed data; and S.C.G. and S.R.P. wrote the paper.

The authors declare no competing interest.

This article is a PNAS Direct Submission.

[1]To whom correspondence may be addressed. Email: rpalli@uky.edu.

This article contains supporting information online at http://www.pnas.org/lookup/suppl/doi:10.1073/pnas.2118871119/-/DCSupplemental.

Published March 8, 2022.

which in turn affected the larval–pupal metamorphosis of *T. castaneum* (13). *HDAC3* knockdown affected the wing development in *T. castaneum* (14). In *G. cornutus*, knockdown of *HDAC1* caused mandible size reduction, whereas *HDAC3* knockdown induced mandible hypertrophy (5). In the brown planthopper, *Nilaparvata lugens*, knockdown of *HDAC1* affected the female and male fertility and ovary development (15). Overexpression of *HDAC4* impaired long-term courtship memory in *D. melanogaster* (16). These studies suggest that each HDAC may perform distinct functions within insect species. However, the role of HDACs in *A. aegypti* growth, development, and metamorphosis are not known. Hence, we investigated the function of HDACs in *A. aegypti* by knocking them down using RNA interference (RNAi). We found that the knockdown of each *HDAC* has a distinct effect on the growth, development, and metamorphosis of *A. aegypti*. The knockdown of *HDAC3* had a severe impact on larval survival, and it is required for maintaining the larval stage in *A. aegypti*.

Results

HDACs Play Distinct Roles in Larval and Pupal Development in *A. aegypti*. To identify the genes coding for HDACs in *A. aegypti*, HDAC protein-coding sequences from *T. castaneum* were used to search the *A. aegypti* genome database. A total 10 HDAC homologs belonging to four classes were identified in *A. aegypti* (*SI Appendix*, Table S1). To determine functions of identified HDACs in *A. aegypti*, these genes were knocked down by feeding second instar larvae on food pellets containing nanoformulated double-stranded RNA (dsRNA targeting each *HDAC* gene. The control larvae were fed on nanoformulated dsRNA targeting the maltose-binding protein gene (*malE*) from *Escherichia coli*. Knockdown of class I HDACs (*HDAC1* and *HDAC3* except for *HDAC8*) affected the larval growth and survival. Specifically, the *HDAC1* knockdown larvae exhibited growth retardation and had smaller bodies than those in control and they eventually died. Although some of the treated larvae developed into pupae, they could not shed their old head capsule and eventually died (Fig. 1). Knockdown of *HDAC3* caused the highest larval mortality; the treated insects remained in the larval stage for an extended period and eventually died (Fig. 1 and *SI Appendix*, Table S2). Knockdown of *HDAC8* affected pupal survival, but no effect on larvae was detected (*SI Appendix*, Table S2). Knockdown of Class II HDACs (*HDAC4* and *HDAC6*) had a moderate impact on larval and pupal survival. *HDAC4* knockdown caused 40% larval mortality, and the remaining larvae pupated but experienced incomplete ecdysis of the head, similar to the phenotype detected in *HDAC1* knockdown (*SI Appendix*, Table S2). *HDAC6* knockdown caused late larval and early pupal mortality. The knockdown of Class III HDACs (Sirtuins 2, 4, 6, and 7) had a major impact on pupal growth and survival. Notably, Sirtuin-2 knockdown increased melanization of pupal cuticle before their death. Knockdown of Sirtuin-4 affected the compound eye development, as the pupae which developed from dsSirtuin-4-treated larvae showed no compound eyes (Fig. 1). Sirtuin-6 and -7 knockdown had low to moderate effects on pupal survival. The knockdown of Class IV HDAC, *HDAC11*, caused moderate larval and high pupal mortality (*SI Appendix*, Table S2). To confirm that the observed phenotype changes are due to the knockdown of target *HDAC* genes, we extracted the total RNA from the treated larvae on the fifth day after dsRNA feeding and determined their messenger RNA (mRNA) levels. We observed more than 55% knockdown of the target *HDAC* genes in respective dsRNA treatments compared to their levels in control larvae fed on a diet containing nanoformulated *dsmalE* (*SI Appendix*, Fig. S1). We also checked whether the dsRNAs used in these experiments have any unintended off-target effects on the other HDAC genes. In this regard, the dsRNA target sequence was aligned with the sequences of the other HDAC genes following the method described recently (17). This alignment did not find any sequences with a continuous stretch of identity between the dsRNA target sequence with the other *HDAC* gene sequences. We also reconfirmed no off-target effects of the selected HDACs dsRNAs by determining relative mRNA levels of other *HDAC* genes in *HDAC3* knockdown larvae (*SI Appendix*, Fig. S2*A*). Similarly, no significant changes in the mRNA levels of *HDAC3* gene were detected in other *HDACs* dsRNAs treated larval samples (*SI Appendix*, Fig. S2*B*). Together, these data suggest that each HDAC has a distinct role in the growth and development of *A. aegypti*; Class I and II HDACs are required for larval growth and development, while Class III and IV HDACs function in pupal and adult development. Among the HDACs tested, *HDAC3* knockdown caused 100% mortality and severe phenotypes; thus, we focused our further studies on HDAC3.

JH Induces the *HDAC3* Expression during the Larval Stage of *A. aegypti*. To understand why *HDAC3* knockdown insects died during the larval stage, *HDAC3* mRNA levels were quantified during larval, pupal, and adult stages of *A. aegypti*. We found that *HDAC3* mRNA levels were higher during larval stages than in other developmental stages. Notably, high *HDAC3* mRNA levels were recorded in the fourth instar larvae up to 30 h after ecdysis to this stage, which then gradually decreased by the end of the larval period (*SI Appendix*, Fig. S3). Moreover, the *HDAC3* mRNA levels showed a positive correlation (R-value: +0.76) with the JH titers during the *A. aegypti* larval stage (18–20), suggesting that JH may induce *HDAC3* expression. To test this hypothesis, we exposed Aag-2 cells to 10 μM of Juvenile hormone III (JH III) for 3 h and quantified the *HDAC3* mRNA levels. Aag-2 cells exposed to JH III showed an increase in *HDAC3* mRNA levels compared to its levels in Aag-2 cells exposed to the control solvent, dimethyl sulfoxide (DMSO) (Fig. 2*A*). Also, newly molted fourth instar larvae grown in water containing 100 ng of JH analog, methoprene, per ml showed significantly higher mRNA levels of *HDAC3* and *Kr-h1* (which is a JH-induced gene—used as a positive control) at 36, 42, and 48 h after molting into fourth instar larvae compared to their expression levels in the control larvae exposed to DMSO (Fig. 2 *B* and *C*). The methoprene-treated larvae died during the pupal stage (*SI Appendix*, Table S3). We also knocked down genes coding for JH acid methyltransferase (*JHAMT*), which is involved in the biosynthesis of JH, and assessed its impact on the expression of *HDAC3*. A significant reduction in the *HDAC3* mRNA levels was detected in the *JHAMT* knockdown larvae (*SI Appendix*, Fig. S4). To confirm that the JH levels were reduced in the *JHAMT* knockdown larvae, the expression of *Kr-h1* (primary JH response gene) was determined. Kr-h1 is sensitive to subnanomolar levels of JH and its expression levels are directly correlated with the JH titers (21, 22). The *Kr-h1* mRNA levels decreased in the *JHAMT* knockdown larvae compared to those in control larvae. These results together confirm that JH induces *HDAC3* expression.

To determine whether JH induces *HDAC3* expression through its receptor, Met, the *Met* gene was knocked down in Aag-2 cells by exposing them to *dsMet* followed by treatment with JH III. The *HDAC3* mRNA levels increased in Aag-2 exposed to *dsmalE* and JH III but not in cells exposed to *dsMet* and JH III (Fig. 2*D*). Moreover, the lowest *HDAC3* mRNA levels were recorded in *Met* knockdown and DMSO-exposed cells compared to its levels in control cells treated with *dsmalE* and DMSO. To reconfirm these results, we transfected Aag-2 cells with *AaMet* expression construct and exposed them to JH III or DMSO. An increase of *HDAC3* mRNA levels was detected in cells transfected with *Met* expression construct and exposed to

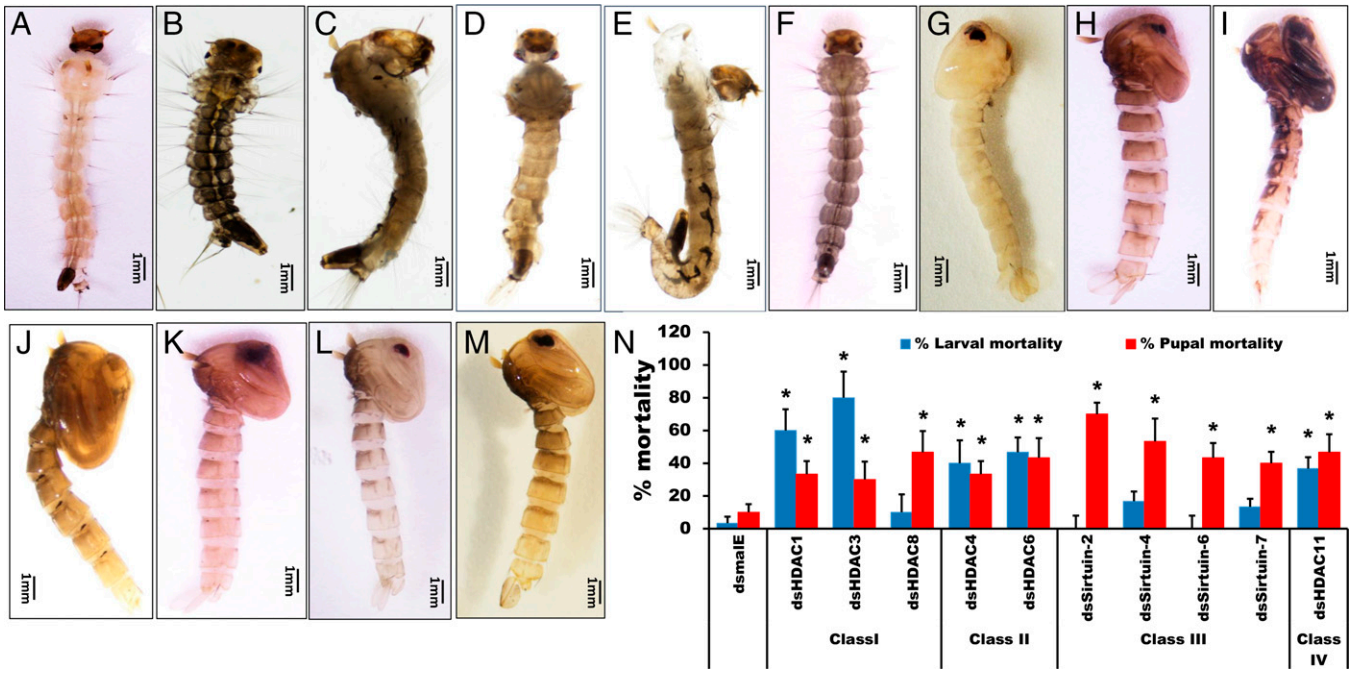

Fig. 1. Knockdown of *HDAC*s affects growth, development, and metamorphosis of *A. aegypti* larvae and pupae. Phenotypes of larvae or pupae fed on food pellets containing nanoformulated dsRNA targeting *HDAC* genes of *A. aegypti*. (*A*) Phenotype of control larvae fed on a *dsmalE*-nanoformulated diet. (*B*) Knockdown of *HDAC1* resulted in larval growth retardation, a decrease in body size and death. (*C*) Some of the *dsHDAC1*-treated larvae pupated, but they were unable to completely shed their old integument and died. (*D*) Knockdown of *HDAC3* caused the highest larval mortality. These larvae stayed in the larval stage for a long period and eventually died. (*E*) Knockdown of *HDAC4* prevented shedding of old integument after metamorphosis into the pupal stage. (*F* and *G*) *HDAC6* knockdown caused late (fourth instar) larval and early pupal mortality. (*H*) *HDAC8* knockdown caused pupal mortality. (*I*) Sirtuin-2 knockdown manifested an increased melanization of pupae before they died. (*J*) Sirtuin-4 knockdown inhibited the compound eye development in the pupae. (*K*) Sirtuin-6 knockdown caused pupal mortality but did not affect larval survival. (*L*) Sirtuin-7 knockdown caused pupal mortality. (*M*) The control larvae fed on a *dsmalE*-nanoformulated diet developed as normal pupae. Scale bar is 1 millimeter in all images. (*N*) Knockdown of *HDAC*s induced larval and pupal mortality in *A. aegypti*. n = 90 (30 × 3 independent experiments). Pupation, adult eclosion rates, and corrected mortality data are included in *SI Appendix*, Table S2.

DMSO. Notably, the *HDAC3* mRNA levels were further increased in Aag-2 cells transfected with *Met* expression construct and exposed to JH III (Fig. 2*E*). These results together confirm that JH induces the *HDAC3* expression through its receptor, Met.

***HDAC3* Knockdown Induces the Expression of Genes Involved in Apoptosis.** Identification of HDAC3 regulated genes and pathways could provide information on its functions and mechanisms involved in the death of *HDAC3* knockdown larvae. Hence, we knocked down *HDAC3* in Aag-2 cells and performed RNA-sequencing (RNA-seq) to identify its targets. The differential gene-expression analysis of RNA-seq data identified 103 up-regulated and 66 down-regulated genes in *HDAC3* knockdown cells compared to their expression levels in control cells treated with *dsmalE* (*SI Appendix*, Fig. S5 and Table S4 and Dataset S1). Gene enrichment analysis revealed that genes involved in apoptosis, postembryonic development, DNA-binding transcription factors, etc. are significantly enriched in the up-regulated gene group (*SI Appendix*, Fig. S6), while Kyoto Encyclopedia of Genes and Genomes (KEGG) pathway enrichment analysis showed that genes involved in Hippo, MAPK, and Notch signaling pathways are significantly enriched in the *HDAC3* knockdown samples (*SI Appendix*, Fig. S7).

To verify the RNA-seq data, we selected 15 up-regulated genes (predicted to be involved in different developmental processes) and determined their expression levels in *HDAC3* knockdown and control larvae using the qRT-PCR. Out of the 15 genes tested, 14 showed similar expression patterns, with the only exception being the gene-coding for mitogen-activated kinase kinase (Fig. 3*A*). Notably, RNA-seq and qRT-PCR data identified one important regulator of apoptosis (ubiquitin regulator of apoptosis, *URA*), which is overexpressed in *HDAC3* knockdown larvae and Aag-2 cells (Fig. 3*A*). URA regulates the inhibitor of apoptosis proteins (IAP), which blocks the activation of caspases and prevents apoptosis (23). Hence, we hypothesized that *HDAC3* knockdown might have altered the expression of genes involved in apoptosis and that might have caused larval death. To test this hypothesis, we determined the mRNA levels of apoptotic genes: *URA*, *IAP*, Anti-IAP protein-Hid, Michelob (reaper), and initiator and executor caspases in *HDAC3* knockdown larvae. The *IAP* mRNA levels were decreased, while *URA*, *Hid*, and the executor caspase 3 mRNA levels were increased in *HDAC3* knockdown larvae (Fig. 3*B*). However, the expression of the Michelob and initiator caspases 8 and 9 were not affected by *HDAC3* knockdown (*SI Appendix*, Fig. S8).

To verify the inverse relationship between the expression of *HDAC3* and its target genes, the developmental expression profiles of *HDAC3*, *URA*, *Hid*, and caspase 3 were determined. A strong negative correlation was observed between *HDAC3* and *URA* (correlation coefficient, R-value: −0.906) and *HDAC3* and *Hid* expression levels (R-value: −0.874) during the larval stage (*SI Appendix*, Fig. S3). Similarly, the expression of *HDAC3* and caspase 3 were negatively correlated (R-value: −0.62059) during the larval stage. These results suggest that HDAC3 is required for suppression of *URA*, *Hid*, and caspase 3 and induction of *IAP*, thereby preventing apoptosis in actively feeding and growing *Ae. aegypti* larvae.

HDAC3 Deacetylates Histone H4 Localized near the Promoters of the Proapoptotic Genes. HDACs suppress target gene expression by deacetylating histones near the promoters of target genes, preventing their access to the transcription machinery. To

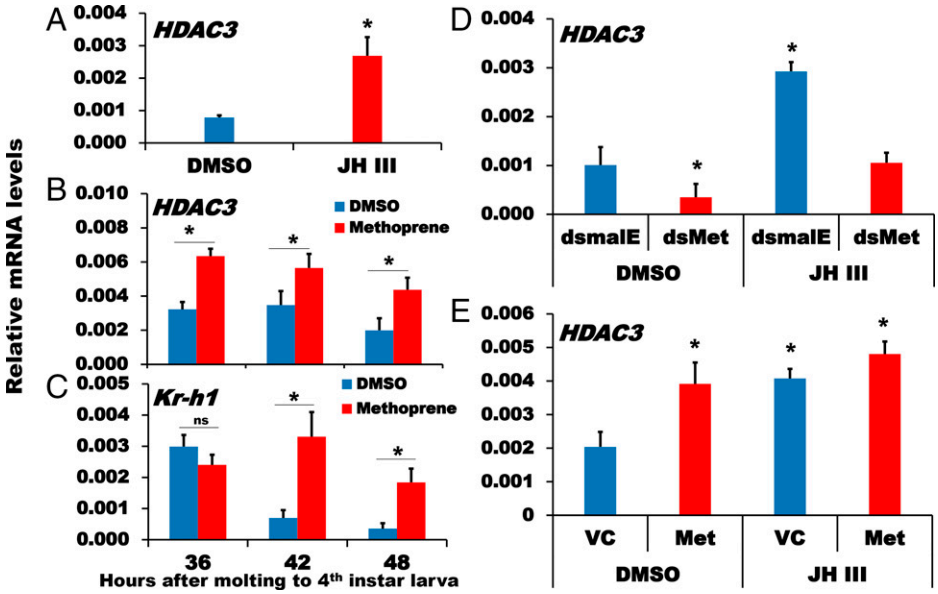

Fig. 2. JH induces *HDAC3* expression through its receptor, Met. (*A*) *HDAC3* expression levels were elevated in Aag-2 cells exposed to 10 μM of JH III compared to its expression levels in control cells exposed to DMSO. (*B*) The expression levels of *HDAC3* in *A. aegypti* larvae treated with 100 ng/mL of JH analog, methoprene, or DMSO. (*C*) *Kr-h1* (used as a positive control) expression levels in methoprene or DMSO-treated larvae. Newly molted fourth instar *A. aegypti* larvae were treated with 100 ng/mL methoprene or DMSO. The *HDAC3* and *Kr-h1* mRNA levels were determined at 36, 42, and 48 h after treatment. (*D*) Knockdown of *Met* in Aag-2 cells prevented JH induction of *HDAC3* expression. (*E*) Overexpression of *Met* receptor in Aag-2 cells induced the *HDAC3* expression. VC: pIEx-4 empty vector control; Met: pIEx-4 vector containing *AaMet* complete ORF. The target gene-expression levels were normalized using the reference gene, *RPS7*, expression levels. Mean + SE (n = 9) are shown. Ns, Not significant. * denotes the significant differences in the expression levels of target genes between treatment and control at $P < 0.05$ analyzed using one-way ANOVA.

determine whether deacetylation of histones is the reason for the altered expression of genes involved in apoptosis, we knocked down *HDAC3* in Aag-2 cells and performed Western blot hybridization using the antibody that detects total lysine acetylation levels. Histone H4 acetylation levels increased in *HDAC3* knockdown cells compared to its acetylation levels in control cells treated with *dsmalE* (Fig. 3*C* and *SI Appendix*, Fig. S9). This result was reconfirmed using the Acetyl-Histone H4 specific antibodies that detect acetylated Ser-1, Lys-5, Lys-8, and Lys-12 amino acids in the N-terminal tail of histone H4 (Fig. 3*C*). To determine whether the HDAC3 deacetylated histone H4 is associated with the promoter regions of genes involved in apoptosis, Aag-2 cells were treated with *dsHDAC3* or *dsmalE* and performed chromatin immunoprecipitation (ChIP) assay using the Acetyl-Histone H4 specific antibody. ChIP assay revealed that key proapoptotic genes, *URA*, *Hid*, and Caspase 3 promoters were enriched in *HDAC3* knockdown cells compared to their promoter enrichment levels in the control cells treated with *dsmalE* (Fig. 3*D*). In contrast, *IAP* and control genes, *β-actin*, and *HSP70* promoters were not enriched in *HDAC3* knockdown cells. These results demonstrate that HDAC3 deacetylates histone H4 localized near the promoters of proapoptotic genes, *URA*, *Hid*, and caspase 3.

HDAC3 and SMRTER Together Suppress the Expression of Genes Involved in Apoptosis. HDAC3 was found to interact with the silencing mediator of retinoid and thyroid hormone receptor (SMRT) to form a corepressor complex that represses the genes regulated by the thyroid hormone receptor (24). The *D. melanogaster* ecdysone receptor–interacting protein, SMRTER, is functionally similar to the vertebrate nuclear corepressors, SMRT and N-CoR (nuclear receptor corepressor) (25). To test whether SMRTER is required for HDAC3 to regulate the expression of genes involved in apoptosis, we knocked down *SMRTER* alone or along with *HDAC3* in Aag-2 cells and quantified the expression of target proapoptotic genes. Interestingly, *SMRTER* knockdown had a similar effect as *HDAC3* knockdown on the expression of the proapoptotic genes (Fig. 3*E* and *SI Appendix*, Fig. S10). The *URA*, *Hid*, and caspase 3 genes were up-regulated in cells exposed to *dsSMRTER* or both *dsSMRTER* and *dsHDAC3* compared to their expression levels in control cells treated with *dsmalE*. Contrastingly, *IAP* mRNA levels were decreased in *dsSMRTER* or both *dsSMRTER*- and *dsHDAC3*-treated cells. Further, to verify whether SMRTER is indeed required for HDAC3 to mediate the suppression of apoptosis genes, we transfected Aag-2 cells with *AaHDAC3* or *AaSMRTER* expression constructs individually or together and determined *URA*, *IAP*, *Hid*, and caspase 3 mRNA levels. The overexpression of *HDAC3* alone did not alter *URA*, *IAP*, *Hid*, and caspase 3 mRNA levels (Fig. 4*A*). However, simultaneous overexpression of *HDAC3* and *SMRTER* in Aag-2 cells resulted in the suppression of *URA*, *Hid*, and caspase 3 genes (Fig. 4*A*). These results suggest that HDAC3 and SMRTER may act cooperatively to suppress apoptosis.

Ecdysone Prevents the *HDAC3*-Mediated Suppression of *URA*, *Hid*, and Caspase 3 Genes. During larval–pupal metamorphosis, JH levels decrease and ecdysone levels increase, which in turn triggers apoptosis of midgut cells (20, 26). To test the influence of ecdysone on *HDAC3* and its target gene expression, Aag-2 cells were exposed to 10 μM of 20-hydroxyecdysone (20E) or DMSO for 3 h, and mRNA levels of *HDAC3* and proapoptotic genes were quantified. The *URA*, *Hid*, and caspase 3 mRNA levels were increased in Aag-2 cells exposed to 20E but not in cells exposed to DMSO (Fig. 4*B*). To confirm this result in in vivo, the 12-h-old fourth instar larvae were treated with 100 ng/mL of stable ecdysone agonist (SEA), and mRNA levels of proapoptotic genes were quantified. The larvae were treated with SEA-induced *URA*, *Hid*, and caspase 3 mRNA levels (Fig. 4*C*), while *HDAC3* mRNA levels were

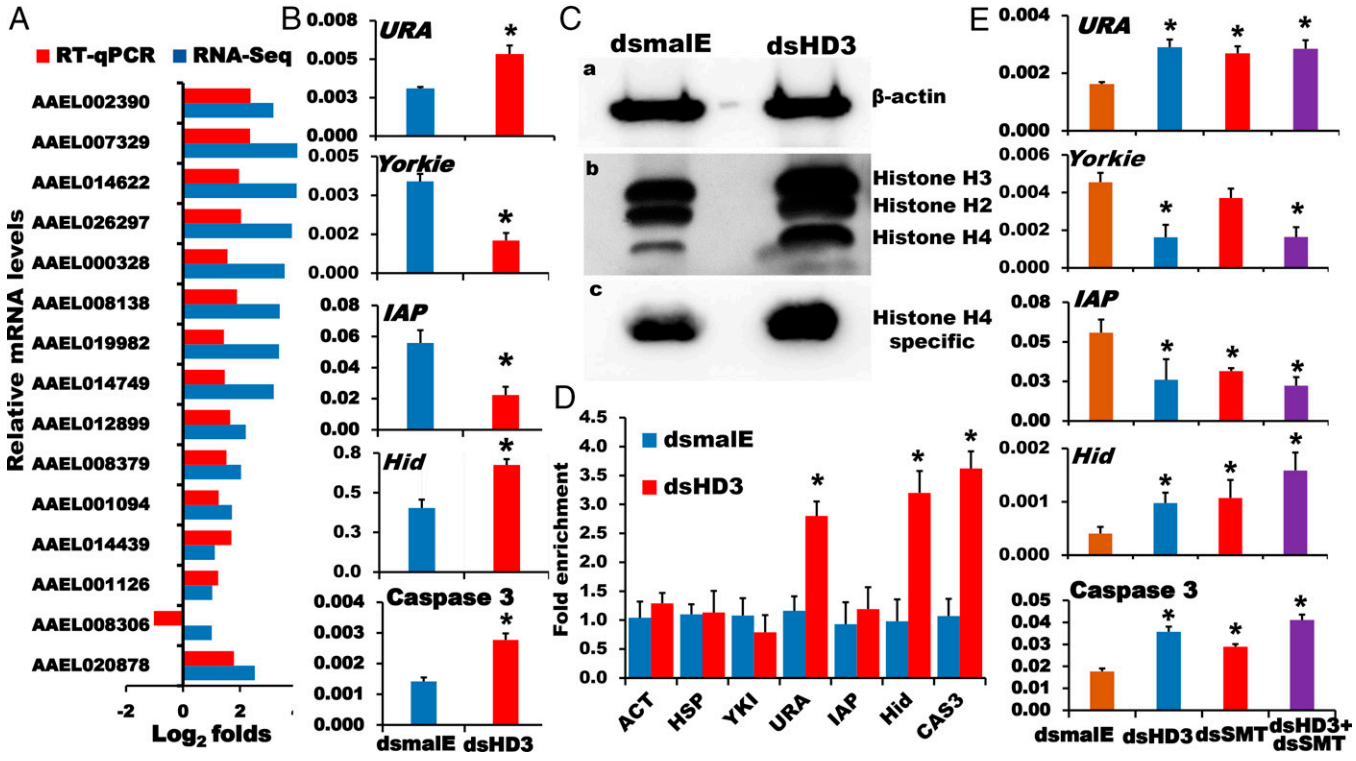

Fig. 3. HDAC3 suppresses apoptosis-triggering gene expression. (*A*) To identify HDAC3 targets and validate their expression, we selected 15 up-regulated genes from the *HDAC3* knockdown RNA-seq data and determined their mRNA levels in the *A. aegypti* larvae fed on a *dsHDAC3*- or *dsmalE*-nanoformulated diet using the RT-qPCR. AAEL002390: Kruppel homolog 1, AAEL007329: Held out wings protein, AAEL014622: Zinc finger transcription factor, AAEL026297: Toll, AAEL000328: Zinc-binding oxidoreductase, AAEL008138: ATP-binding cassette G1, AAEL019982: Ras GTPase-activating protein, AAEL014749: Ras-related protein, AAEL012899: Meiotic nuclear division protein 1, AAEL008379: Mitogen-activated kinase 14B, AAEL001094: Heat shock protein beta-1, AAEL014439: Juvenile hormone-inducible protein, AAEL001126: REST corepressor, AAEL008306: Mitogen-activated kinase kinase 15 (MAP3K15), and AAEL020878: Ubiquitin regulator of apoptosis (*URA*). (*B*) Knockdown of *HDAC3* in *A. aegypti* larvae induced the expression of genes involved in apoptosis. The mRNA levels of *URA*, *Yorkie*, *Hid*, *IAP*, and cell death enzyme, caspase 3, were determined in the *A. aegypti* larvae fed on *dsHDAC3*-nanoformulated diet and the control larvae fed on *dsmalE*-nanoformulated diet. (*C*) HDAC3 deacetylates histone H4—acetylation levels were determined by Western blot using the proteins from Aag-2 cells treated with *dsHDAC3* or *dsmalE* (control). (a) β-actin (used as a loading control) levels in *dsHDAC3*- or *dsmalE*-treated cells. (b) Histone H2, H3, and H4 acetylation levels in *dsHDAC3*- or *dsmalE*-treated cells detected using the Acetylated-Lysine (Ac-K2-100) MultiMab Rabbit mAb mix. (c) Histone H4 acetylation levels were detected using the Ac-Histone H4 specific mAb antibody (E-5). (*D*) ChIP assay revealed that knockdown of *HDAC3* enriched the histone H4 acetylation levels at the promoter regions of *URA*, *Hid*, and caspase 3. Aag-2 cells were treated with *dsmalE* or *dsHDAC3* for 72 h. The chromatin was cross linked and enriched using the Ac-Histone H4 specific mAb antibody (E-5). Purified DNA was used in qPCR to quantify the enrichment levels of promoters of target genes and control genes, *β-actin* and *HSP70*. Normalization was performed using the Rabbit IgG antibody–enriched chromatin DNA (negative control). Data are shown as fold enrichment mean ± SE (n = 8). * denotes significant differences in the promoter enrichment levels between treatment and control analyzed using one-way ANOVA at $P < 0.005$. (*E*) Both HDAC3 and SMRTER regulate the expression of genes involved in apoptosis. The mRNA levels of *URA*, *Yorkie*, *Hid*, *IAP*, and caspase 3 were determined in the Aag-2 cells exposed individually to *dsHDAC3*, *dsSMRTER*, or both *dsHDAC3* and *dsSMRTER*. The target gene-expression levels were normalized using the reference gene, *RPS7*, expression levels. Mean + SE (n = 9) are shown. * denotes the significant differences in the mRNA levels of target genes between treatment and control at $P < 0.05$ analyzed using one-way ANOVA. dsHD3, *dsHDAC3*; *dsSMT*, *dsSMRTER*; ACT, β-Actin; and YKI, *Yorkie*. *HDAC3* and *SMRTER* expression levels in the cognate dsRNA treatments are provided in *SI Appendix*, Fig. S10.

not affected by 20E or SEA treatments in Aag-2 cells or *A. aegypti* larvae, respectively. Next, to test whether the presence of JH III has any influence on the 20E induction of *URA*, *Hid*, and caspase 3 genes, Aag-2 cells were simultaneously exposed to both 20E and JH III, and mRNA levels of proapoptotic genes were determined. Notably, 20E induced *URA*, *Hid*, and caspase 3 mRNA levels even in the presence of JH III (Fig. 4*B*). Similarly, an increase in *URA*, *Hid*, and caspase 3 mRNA levels were observed in *A. aegypti* larvae simultaneously exposed to both SEA and methoprene (Fig. 4*C*). Further, to determine the effect of 20E on HDAC3- and SMRTER-mediated suppression of *URA*, *Hid*, and caspase 3 genes, Aag-2 cells were transfected with both *AaHDAC3* and *AaSMRTER* expression constructs and exposed to 20E or DMSO. In DMSO-exposed Aag-2 cells overexpressing *AaHDAC3* and *AaSMRTER*, suppression of *URA*, *Hid*, and caspase 3 genes were observed (Fig. 4*A*). However, 20E blocked *AaHDAC3*- and *AaSMRTER*-mediated suppression of *URA*, *Hid*, and caspase 3 genes. These results suggest that HDAC3 and SMRTER suppress *URA*, *Hid*, and caspase 3 genes in the presence of JH, but 20E prevents HDAC3- and SMRTER-mediated suppression of proapoptotic genes.

HDAC3 Regulates Midgut Cell Apoptosis Independent of Ecdysone Response Genes, *E93* (Adult Specifier), and Broad Complex (Pupal Specifier). Previous studies showed that the overexpression of the primary ecdysone response gene, *E93*, induces apoptosis in midgut cells during metamorphosis (27). To determine whether *HDAC3* knockdown–induced midgut cell apoptosis is mediated through E93, the expression levels of *E93* and genes coding for broad complex (*Br-C*) isoforms were analyzed in *HDAC3* knockdown larvae. The *E93* and *Br-C* mRNA levels were lower in *HDAC3* knockdown larvae when compared to their levels in control larvae treated with *dsmalE* (*SI Appendix*, Fig. S11). These data suggest that HDAC3 independently regulates the genes involved in apoptosis to control midgut cell apoptosis.

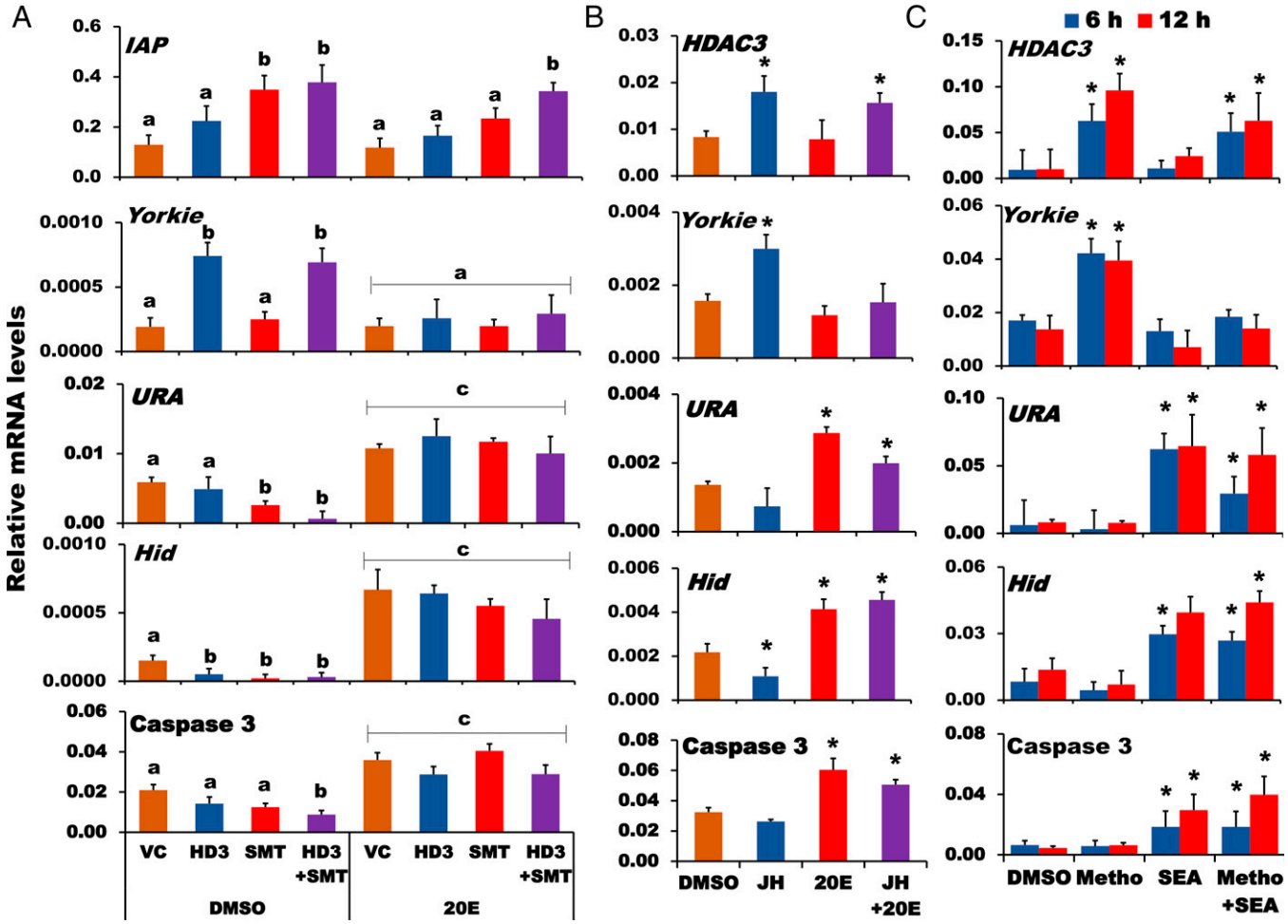

Fig. 4. HDAC3- and SMRTER-mediated suppression of apoptosis genes is prevented by 20E. (*A*) Overexpression of both *AaHDAC3* and *AaSMRTER* in Aag-2 cells suppresses *URA*, *Hid*, and caspase 3 and induces *IAP* and *Yorkie* expression. The HDAC3- and SMRTER-mediated suppression of *URA*, *Hid*, and caspase 3 genes in Aag-2 cells is blocked by 20E. Error bars show the SE mean of the four biological replicates. Bars with the same letter are not significantly different at 95% CI. (*B*) Presence of 20E induces the expression of *URA*, *Hid*, and caspase 3 genes but does not affect the expression of *HDAC3* and *Yorkie* in Aag-2 cells. JH III induced the expression of *HDAC3* and *Yorkie* in Aag-2 cells. However, Aag-2 cells simultaneously exposed to both JH III and 20E hormones revealed that JH was unable to suppress the proapoptotic genes, *URA*, *Hid*, and caspase 3 expressions in the presence of ecdysone. (*C*) SEA induces the expression of *URA*, *Hid*, and caspase 3 genes but no effect on the expression of *HDAC3* and *Yorkie*. JH analog, Methoprene, induces the expression of *HDAC3* and *Yorkie*. Fourth instar larvae 12 h old were treated individually with 100 ng/mL of methoprene, SEA, or a mix of both hormone analogs. The mRNA levels of target genes were determined at 6 and 12 h after treatment. The target gene-expression levels were normalized using the reference gene, *RPS7*, expression levels. Mean + SE (n = 9) are shown. * denotes the significant differences in the mRNA levels of target genes between treatment and control at $P < 0.05$ analyzed using one-way ANOVA. JH III, Juvenile hormone III; 20E, 20-hydroxyecdysone; DMSO, Dimethyl sulfoxide; SEA, Stable ecdysone agonist (RH-102240); HD3, *HDAC3* overexpression; and SMT, *SMRTER* overexpression.

Midgut Size Is Reduced in *HDAC3* Knockdown Larvae. To determine whether apoptosis is the cause of larval death in *HDAC3* knockdown larvae, the larval alimentary canals were dissected from 42-h-old fourth instar larvae that fed on *dsHDAC3* or *dsmalE* and observed under a microscope. *HDAC3* knockdown and control larvae exhibited a similar body size (Fig. 5*A* and *SI Appendix*, Fig. S12). However, a shorter alimentary canal was detected in *HDAC3* knockdown larvae compared to its size in the control larvae (Fig. 5*B*). To identify which part of the alimentary canal size was reduced in *HDAC3* knockdown larvae, the experiment was repeated with *A. aegypti* larvae expressing the enhanced green fluorescent protein (EGFP) under IE1-hr5 promoter-enhancer and DsRed (Discosoma red fluorescent) protein driven by the IE2 promoter. The second instar larvae of this strain were fed on food pellets containing nanoformulated *dsHDAC3* or *dsmalE*. The alimentary canals were dissected at 42 h after molting into fourth instar larvae and observed under a fluorescence microscope. As shown in Fig. 5*C*, the midgut of *dsHDAC3*-treated larvae is significantly shorter than in the control larvae treated with *dsmalE*. Further, TUNEL (Terminal deoxynucleotidyl transferase dUTP nick end labeling) assay was used to identify apoptotic cells in the larval midguts dissected from the fourth instar larvae that fed on *dsHDAC3* or *dsmalE*. Midgut cells undergoing apoptosis (as indicated by the green fluorescence of fragmented nuclear DNA labeled with fluorescent dUTP) were detected in 12-h-old fourth instar larvae, which fed on the *dsHDAC3*-containing diet (Fig. 5*D*). Moreover, the number of fluorescent nuclei increased in 24-h-old larvae, and this number continued to increase until 48 h after molting into the fourth instar larvae that fed on the *dsHDAC3*-containing diet. Meanwhile, the control larvae which fed on *dsmalE*-containing diet showed fluorescently labeled nuclei only at 48 h after molting into fourth instar larvae. Moreover, the number of fluorescently labeled nuclei detected is lower

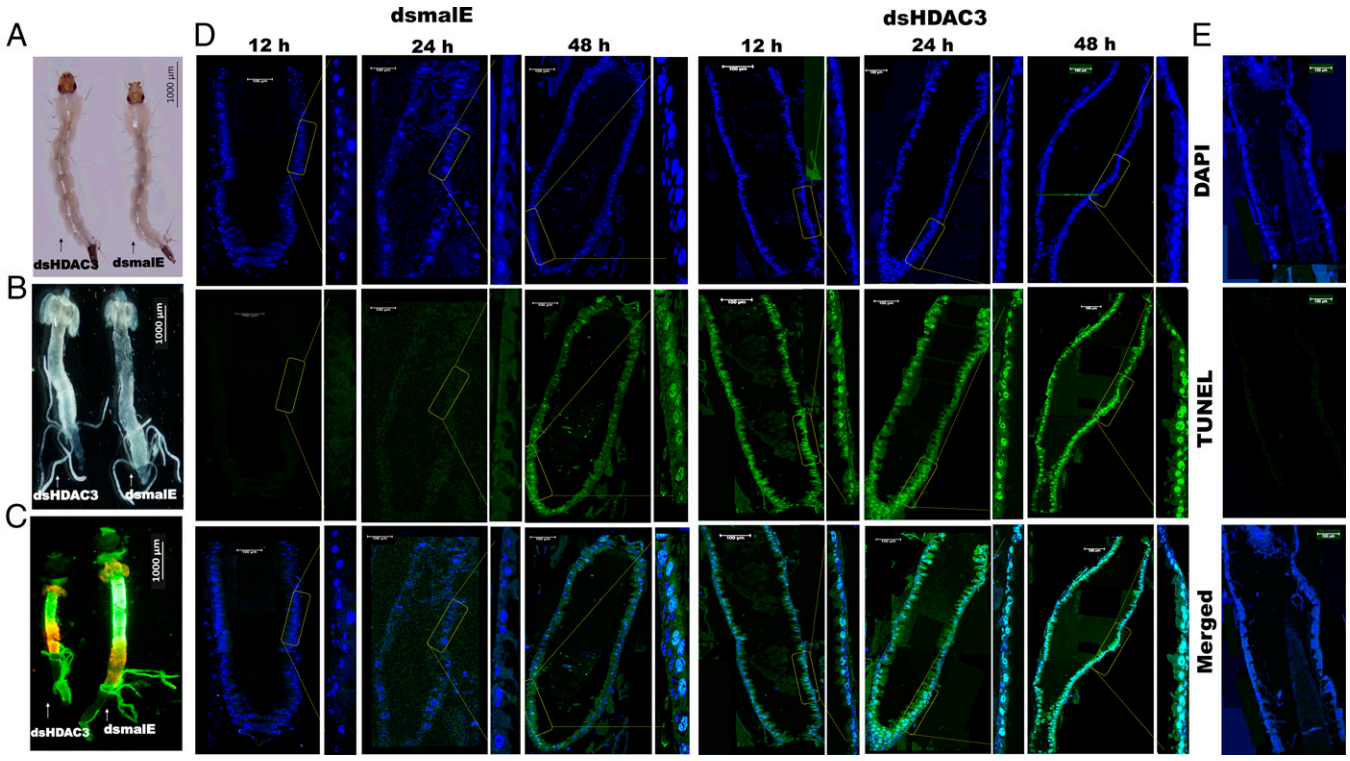

Fig. 5. Knockdown of *HDAC3* induces apoptosis, resulting in midgut size reduction in *A. aegypti* larvae. (*A*) *HDAC3* knockdown and control larvae are similar in size. (*B*) The alimentary canals in *HDAC3* knockdown larvae are shorter than those in the control larvae. The alimentary canals were dissected at 42 h after molting into fourth instar larvae fed on *dsHDAC3*- or *dsmalE*-nanoformulated diet. The alimentary canals were visualized under a fluorescence microscope using a white filter. (*C*) The alimentary canals in *HDAC3* knockdown larvae expressing EGFP and DsRed are shorter than those in the control larvae fed on *dsmalE*. The alimentary canals were dissected 42 h after molting into fourth instar larvae. These alimentary canals were observed under a fluorescence microscope using the GFP filter. (Scale bar, 1,000 μm). (*D*) *HDAC3* knockdown triggered apoptosis of midgut cells. Longitudinal sections 4 μM thick were cut from the midgut dissected from *dsHDAC3*- or *dsmalE*-treated larvae at 12, 24, and 48 h after ecdysis to the fourth instar larval stage. The sections were stained with the TUNEL assay reagent and DAPI nuclear stain and photographed under a confocal microscope. (*E*) No background green fluorescence was detected in the control larval section stained only with DAPI without TUNEL reaction mixture. (Scale bar, 100 μm.) The larval body and alimentary canal sizes and the mean fluorescence intensity values of apoptotic cells are provided in *SI Appendix*, Fig. S12.

than those in *HDAC3* knockdown larvae (Fig. 5*D* and *SI Appendix*, Fig. S12). These results demonstrate that *HDAC3* knockdown induces apoptosis of midgut cells in feeding larvae and causes a decrease in midgut size.

Discussion

One of the major contributions of this paper is the discovery that HDACs are important players in the regulation of growth, development, and metamorphosis of *A. aegypti*. Interestingly, the knockdown of each *HDAC* gene showed a distinct effect on the growth, development, and metamorphosis of *A. aegypti*. Out of the 10 *HDAC* genes tested, knockdown of *HDAC3* showed the most-severe phenotypes during the larval stages, suggesting that it is required for maintaining the larval stage in *A. aegypti*. Our previous studies in *T. castaneum* also showed that HDACs have distinct functions (13). The knockdown of *HDAC3* affected the wing development, and *HDAC1* knockdown showed the most-severe phenotypes in *T. castaneum* (14). The developmental expression pattern of *AaHDAC3* suggests its major role during the larval stage of *A. aegypti*. Moreover, *HDAC3* mRNA levels correlate with JH titers during the larval stage, and JH induces *HDAC3* expression through its receptor, *Met*. In our previous studies, JH suppressed the expression of *HDAC1*, *HDAC3*, and *HDAC11* in *T. castaneum*, suggesting that the JH regulation of HDACs is different between *A. aegypti* and *T. castaneum* (13, 14, 28). In the current study, we also identified conserved JH response elements in the promoter region (−815 to −803 bp) of the *HDAC3* gene, suggesting that the JH receptor complex may bind to the upstream region of *HDAC3* and induce its expression in the presence of JH, which is similar to JH induction of *Kr-h1* and other JH response genes (21, 22, 29–31). However, further studies are required to test binding of the Met complex to the upstream region of *HDAC3*.

Studies in mammalian systems suggest that HDAC3 activity is influenced by its association with the corepressors, SMRT and N-CoR (32). Here, we report that transcriptional repression of apoptosis genes by HDAC3 requires SMRTER, which is functionally similar to the vertebrate nuclear corepressors; SMRT and N-CoR. SMRTER may be recruited to proapoptotic gene promoters and serve as an anchoring molecule for recruiting HDAC3 (*SI Appendix*, Fig. S13). The recruited HDAC3 could deacetylate histones resulting in the suppression of proapoptotic gene expression. Previous studies showed that the interaction of SMRT/N-CoR with HDAC3 potentiates HDAC3 activity (32). Similarly, we found that overexpression of *HDAC3* alone is not sufficient to suppress the expression of the *URA*, *Hid*, and caspase 3. However, simultaneous overexpression of both *HDAC3* and *SMRTER* suppressed these genes, suggesting that SMRTER is required for HDAC3 action.

We observed a decreased midgut size in the *HDAC3* knockdown larvae, perhaps due to the premature death of midgut cells. HDAC3 was shown to be involved in suppressing genes involved in apoptosis (32). Apoptosis is initiated after decreased expression of antiapoptotic genes such as *IAP* and increased expression

of proapoptotic genes such as *Hid* and caspases. In our study, knockdown of *HDAC3* induced the overexpression of *URA*, *Hid*, and caspase 3 genes and suppressed expression of *IAP*. We showed that *HDAC3* knockdown increased acetylation of histone H4 near the promoters of *URA*, *Hid*, and caspase 3 genes, suggesting that HDAC3 regulates the expression of these genes through chromatin modifications. In contrast, the acetylation levels of H4 near the *IAP* promoter were not affected by *HDAC3* knockdown, suggesting that HDAC3 may not directly affect *IAP* gene expression. RNA-seq analysis revealed that the Hippo-signaling pathway is enriched in *HDAC3* knockdown cells (*SI Appendix*, Fig. S7). Hippo-signaling controls growth and development in *D. melanogaster* and mammals by regulating the tumor suppressor genes (33). Hippo-signaling dysfunction induces a growth-promoting oncogene, *Yorkie*, which is known to induce the *IAP* expression. Notably, HDAC3 is required for *Yorkie* expression (Fig. 4). Therefore, *HDAC3* knockdown might have increased Hippo-signaling that resulted in the suppression of *Yorkie* and its downstream regulator, *IAP* (Fig. 3).

The other apoptosis protein, Hid, is also induced by the *HDAC3* knockdown. Hid binds to IAP and blocks its action. It is also possible that URA induced by *HDAC3* knockdown may regulate IAP protein activity by cleaving it to prevent IAP binding to caspases (23). In the absence of IAP, the initiator caspase 9 undergoes autocatalytic processing and becomes active. *HDAC3* knockdown also induced hyperacetylation of the caspase 3 promoter that results in increased caspase 3 levels. The activated initiator caspase 9 cleaves the interchain of the inactive caspase 3 to make it catalytically active. Activated caspase 3 degrades many cellular proteins and causes apoptosis. Previous studies showed that inhibition of HDACs activity decreased cholangiocarcinoma cell growth and increased caspase-dependent apoptosis (34, 35).

Interestingly, caspase 3 was shown to cleave the C-terminal region of HDAC3 (which results in loss of its activity) and nuclear localization signal peptide (that leads to accumulation of HDAC3 protein in the cytoplasm) (36). The truncated HDAC3 was unable to deacetylate histones associated with proapoptotic gene promoters. Then URA-mediated ubiquitin-dependent degradation of HDAC3 results in the induction of caspase 3-mediated apoptosis (36). A previous study demonstrated that blocking of DPP-signaling induces autophagy in midgut cells and eventually removes midgut cells (37), while application of JH analog, methoprene, prevents apoptosis of larval midgut cells during larval–pupal metamorphosis and retains larval midgut in *A. aegypti* pupae (38). In this study, we showed that JH-induced, HDAC3-mediated deacetylation suppresses proapoptotic genes during the larval stage to prevent premature induction of apoptosis in larval midgut cells.

During larval–pupal metamorphosis, a decrease in JH titers and an increase in ecdysteroid titers may cause an exchange of the corepressor complex with a coactivator complex near the ecdysone response gene promoters to activate their transcription (39). We observed that HDAC3 was unable to suppress genes involved in apoptosis in the presence of 20E. This suggests that 20E acts as a switch to induce proapoptotic genes by exchanging corepressor complex (SMRTER/HDAC3) with a coactivator complex and recruiting ecdysone receptors to the promoters of these genes (40–42). This leads to transcription of proapoptotic genes and apoptosis of larval midgut (*SI Appendix*, Fig. S13). Similarly, in the absence of ligand, thyroid hormone, retinoic acid receptors recruit SMRT/N-CoR corepressor complexes that bind to the target gene promoters and repress gene transcription. However, the presence of thyroid hormone dissociates corepressor complexes and recruits coactivator complexes to the promoters to induce target gene expression (43).

In conclusion, we showed that antagonistic actions of JH and ecdysone on proapoptotic gene expression are mediated by the HDAC3 complex. JH induces an epigenetic modifier, *HDAC3*, to prevent premature death of larval cells during the feeding stage. During metamorphosis, the decline in JH titers and increase in ecdysone titers result in the suppression of HDAC3 and promotion of apoptosis of larval midgut cells. This study could serve as a foundation for understanding the role of epigenetic modifications in the antagonistic action of JH and ecdysone involved in the regulation of the expression of apoptosis genes during larval development and metamorphosis.

Materials and Methods

Larval Bioassays. *A. aegypti* Liverpool (LVP) strain mosquitoes were reared as described previously (9). To knockdown target genes, dsRNA was synthesized using the MEGAscript RNAi kit (Life Technologies) as described previously (44). Poly-L-lysine (PLL):Epigallocatechin gallate (EGCG):dsRNA nanoparticle complexes were prepared following the methods described previously (9, 45). Briefly, food pellets were prepared by mixing PLL:EGCG:dsRNA complexes with mosquito larval food and bovine liver powder. These pellets were fed to second instar larvae in 12-well plates (five larvae/well; n = 30) containing 2 mL nuclease-free water. Each food pellet contained 40 μg dsRNA conjugated with PLL:EGCG nanoparticles. Each food pellet was divided into three equal pieces and distributed to three wells. Fresh food pellets containing PLL:EGCG:dsRNA complexes were added to each well every day until pupation or death. Mortality and phenotypes were recorded every day until adult eclosion. Corrected mortality was calculated using Abbott's formulae (46).

Cell Culture, Target Gene Knockdown, and Hormone Treatment. *A. aegypti* embryo-derived Aag-2 cells were cultured at 28 °C in Schneider's *Drosophila* medium (Life Technologies) supplemented with 10% fetal bovine serum (Life Technologies). Aag-2 cells were seeded in 6-well culture plates at a density of 200,000 cells/well. Cells were treated with 10 μg dsRNA of target or *dsmalE* (control) for 3 consecutive d. On the fourth day, cells were exposed to 10 μM of JH III (Sigma-Aldrich) or 20E (Sigma-Aldrich) or DMSO for 3 h. Then the total RNA was isolated, and target genes mRNA levels were quantified.

JH Analog, Methoprene, and Ecdysone Agonist Treatments. Technical-grade methoprene (isopropyl (E,E)-(RS)-11-methoxy-3,7,11-trimethyldodeca-2,4-dienoate) was dissolved in DMSO. Technical-grade SEA, RH-102240 (N-(1,1-dimethylethyl)-N¢-(2-ethyl-3-methoxybenzoyl)-3,5-dimethylbenzohydrazide) was dissolved in ethanol. In total, 100 ng/mL final concentration of methoprene or SEA was added to nuclease-free water and dispensed into 12-well plates and released newly molted five fourth instar larvae/well (n = 20: four replicates). Control larvae were treated with 1 μL/mL DMSO or ethanol. RNA was extracted from the treated and control larvae at 36, 42, and 48 h after treatment.

RNA Isolation, cDNA Preparation, and qRT-PCR. Total RNA was extracted from *A. aegypti* larvae or pupae or Aag-2 cells using the TRI reagent by following the manufacturer's protocol (Molecular Research Center, Inc.). Developmental expression of target genes was determined by extracting the total RNA from the whole insects collected at different time points during development. First-strand complementary DNA (cDNA) synthesis using 2 μg total RNA and qRT-PCR assays were performed as described previously (9). *RPS7* and *β-tubulin* housekeeping genes were used as internal reference genes to normalize the target gene mRNA levels (*SI Appendix*, Table S5). The target gene-expression levels were normalized with the reference gene-expression levels by subtracting the target gene C_T value from the reference gene C_T value followed by determination of $-\Delta\Delta C_T$ value (47). All experiments were performed using at least three biological replicates and repeated three times.

RNA-Seq and Annotation. Three RNA-seq libraries per treatment were prepared using RNA isolated from three independent biological samples of Aag-2 cells treated with *dsHDAC3* or *dsmalE*. KAPA Stranded mRNA-Seq Kit (Illumina) was used to prepare RNA-seq libraries by following manufacturer protocol. RNA-seq was performed using the Illumina HiSeq 4000 sequencer platform (Sequencing and Genomics Technologies Center of Duke University). RNA-seq data were analyzed using the CLC Genomics Workbench (version 10.1.1, Qiagen Bioinformatics) as described previously (44). Briefly, the sequence data were subjected to quality control to remove low-quality reads and adapters. Clean reads were mapped to the LVP strain transcriptome data retrieved from VectorBase (https://vectorbase.org/vectorbase/app/record/dataset/TMPTX_aaegLVP_AGWG). Mapping was performed using the CLC Genomics Workbench employing default mapping parameters. To find the differentially expressed genes between *dsHDAC3* treatment and *dsmalE*-treated control, the empirical analysis of the differential gene-expression tool

in the CLC Genomics Workbench was used by employing standard parameters along with greater- or equal-than-twofold expression variation and a P value < 0.05 cutoff values. For annotation, the cloud blast feature in the Blast2GO software was used to check against the arthropod nonredundant protein database with a Blast expectation value (e-value) 1.0×10^{-6}. Gene Ontology (GO) enrichment analysis was performed using the Web Gene Ontology Annotation Plot (WEGO) online tool (48). KEGG pathway enrichment analysis was performed using the KEGG Orthology-Based Annotation System (KOBAS) 3.0 online tool (49).

Western Blot Hybridization and ChIP Assay. To identify HDAC3 deacetylated histones, Aag-2 cells were treated with *dsHDAC3* or *dsmalE* for 3 consecutive d, and chromatin-bound proteins were isolated by following the protocol described previously (50). Western blotting was performed using 10 μg total protein resolved on 12% SDS-PAGE (sodium dodecyl sulfate–polyacrylamide gel electrophoresis) gels. Blotting, hybridization, and detection were carried out as described previously (9). Band intensities of three replicate Western blots were measured using the ImageJ software, and statistical analysis was performed to determine the significance of difference (18).

ChIP assays were performed using the Pierce Magnetic ChIP Kit (Thermo Fisher Scientific) as described previously (9). Briefly, 2×10^6 cells were treated with 10 μg *dsHDAC3* or *dsmalE* for 3 consecutive d. On the fourth day, cells were cross linked using formaldehyde. Cross-linked DNA was digested with micrococcal nuclease and immunoprecipitated using antibodies that recognize histone H4 acetylation (Ac-Histone H4 Antibody [E-5]: sc-377520; Santa Cruz Biotechnology, Inc., Dallas) or the rabbit IgG antibody (used as a negative control). Immunoprecipitated DNA was purified, and the target genes promoter enrichment levels were quantified using the qPCR.

Transfection and Overexpression of Target Genes. To overexpress *AaMet* in Aag-2 cells, the *AaMet* construct reported previously was used (21). Full-length *AaHDAC3* and *AaSMRTER* cDNAs were cloned into the pIEx-4 vector and used for transfection. Aag-2 cells were transfected with 500 ng of pIEx-4 vector containing the gene of interest or empty pIEx-4 vector (control) using the Cellfectin II transfection reagent. At 48 h after transfection, the cells were exposed to DMSO or 10 μM of JH III or 20E for an additional 3 h. Total RNA was isolated from these cells used to quantify mRNA levels of target genes. Three independent experiments were performed, and each experiment included four biological replicates.

Preparation of Whole-Insect Longitudinal Sections and TUNEL Assay. TUNEL assays were performed on whole-insect longitudinal sections as described previously (38). Briefly, alimentary canals were dissected from larvae that fed on *dsHDAC3*- or *dsmalE*-nanoformulated diet, then washed with 1× phosphate-buffered saline (PBS) and fixed in 4% paraformaldehyde overnight at 4° C. After fixation, the tissues were washed with 1× PBS twice, then dehydrated using a series of grades of ethanol (25%, 50%, 75%, 95%, and 100% in 1× PBS) and infiltrated through a series of grades of xylene (25%, 50%, 75%, 95%, and 100% in ethanol) and embedded in Paraplast Plus at 56° C. Longitudinal sections 4 μM thick were cut using a microtome (Leica RM 2135, Germany) and mounted on a glass slide. The sections were deparaffinized by incubating glass slides at 60° C for 1 h, followed by rehydration using a series of grades of xylene and ethanol. Then the sections were incubated in 0.3% Triton X-100 in 0.1% sodium citrate buffer for 10 min and washed with 1× PBS twice and used to perform TUNEL assay using the In Situ Cell Death Detection Kit, Fluorescein (Roche) by following manufacturer's instructions. Sections were exposed to the TUNEL reaction mixture (30 μl/slide) for 60 mins at 37° C, then washed with 1× PBS and mounted using DAPI nuclear-staining reagent. The sections were examined under the Leica TCS SP8 DLS (Digital LightSheet) confocal microscope. The mean fluorescence intensities for control and treated samples were determined by following the method described by Shihan et al. (51).

Statistical Analysis of Data. One-way ANOVA was used for all statistical analysis unless otherwise stated. $P < 0.05$ was considered significant.

Data Availability. The RNA-seq data have been deposited to the National Center for Biotechnology Information's Sequence Read Archive with accession no. PRJNA746176.

ACKNOWLEDGMENTS. This work was supported by a grant from NIH (GM070559) to S.R.P. Thanks to Dr. Xien Chen and Dr. Kim Kyungbo for providing plasmid constructs and Dr. Guan-Heng Zhu for providing the EGFP-DsRed–expressing transgenic line of *A. aegypti*. We also thank Jeff Howell for help with insect-rearing and editing the manuscript.

1. J. E. Crawford *et al.*, Population genomics reveals that an anthropophilic population of *Aedes aegypti* mosquitoes in West Africa recently gave rise to American and Asian populations of this major disease vector. *BMC Biol.* **15**, 16 (2017).
2. K. M. Glastad, B. G. Hunt, M. A. D. Goodisman, Epigenetics in insects: Genome regulation and the generation of phenotypic diversity. *Annu. Rev. Entomol.* **64**, 185–203 (2019).
3. D. Kirilly *et al.*, Intrinsic epigenetic factors cooperate with the steroid hormone ecdysone to govern dendrite pruning in Drosophila. *Neuron* **72**, 86–100 (2011).
4. A. Spannhoff *et al.*, Histone deacetylase inhibitor activity in royal jelly might facilitate caste switching in bees. *EMBO Rep.* **12**, 238–243 (2011).
5. T. Ozawa *et al.*, Histone deacetylases control module-specific phenotypic plasticity in beetle weapons. *Proc. Natl. Acad. Sci. U.S.A.* **113**, 15042–15047 (2016).
6. D. F. Simola *et al.*, Epigenetic (re)programming of caste-specific behavior in the ant *Camponotus floridanus*. *Science* **351**, aac6633 (2016).
7. J. E. Leader, C. Wang, M. Fu, R. G. Pestell, Epigenetic regulation of nuclear steroid receptors. *Biochem. Pharmacol.* **72**, 1589–1596 (2006).
8. K. Mukherjee, R. Fischer, A. Vilcinskas, Histone acetylation mediates epigenetic regulation of transcriptional reprogramming in insects during metamorphosis, wounding and infection. *Front. Zool.* **9**, 25 (2012).
9. S. C. Gaddelapati, R. K. Dhandapani, S. R. Palli, CREB-binding protein regulates metamorphosis and compound eye development in the yellow fever mosquito, *Aedes aegypti*. *Biochim. Biophys. Acta. Gene Regul. Mech.* **1863**, 194576 (2020).
10. A. Roy, S. George, S. R. Palli, Multiple functions of CREB-binding protein during post-embryonic development: Identification of target genes. *BMC Genomics* **18**, 996 (2017).
11. J. Xu, A. Roy, S. R. Palli, CREB-binding protein plays key roles in juvenile hormone action in the red flour beetle, *Tribolium Castaneum*. *Sci. Rep.* **8**, 1426 (2018).
12. S. R. Palli, Epigenetic regulation of post-embryonic development. *Curr. Opin. Insect Sci.* **43**, 63–69 (2021).
13. S. George, S. C. Gaddelapati, S. R. Palli, Histone deacetylase 1 suppresses Krüppel homolog 1 gene expression and influences juvenile hormone action in *Tribolium castaneum*. *Proc. Natl. Acad. Sci. U.S.A.* **116**, 17759–17764 (2019).
14. S. George, S. R. Palli, Histone deacetylase 3 is required for development and metamorphosis in the red flour beetle, *Tribolium castaneum*. *BMC Genomics* **21**, 420 (2020).
15. J. L. Zhang *et al.*, The histone deacetylase NlHDAC1 regulates both female and male fertility in the brown planthopper, *Nilaparvata lugens*. *Open Biol.* **8**, 180158 (2018).
16. H. L. Fitzsimons, S. Schwartz, F. M. Given, M. J. Scott, The histone deacetylase HDAC4 regulates long-term memory in Drosophila. *PLoS One* **8**, e83903 (2013).
17. J. Chen *et al.*, Off-target effects of RNAi correlate with the mismatch rate between dsRNA and non-target mRNA. 10.1080/15476286.2020.1868680 (2021).
18. S. Hernández-Martínez, C. Rivera-Perez, M. Nouzova, F. G. Noriega, Coordinated changes in JH biosynthesis and JH hemolymph titers in *Aedes aegypti* mosquitoes. *J. Insect Physiol.* **72**, 22–27 (2015).
19. L. M. Riddiford, "2 - Hormone Action at the Cellular Level" *in Endocrinology II*, G. A. Kerkut, L. I. Gilbert, Eds. (Pergamon, Amsterdam, 1985), pp. 37–84, 10.1016/B978-0-08-030809-8.50008-3.
20. J. W. Truman, L. M. Riddiford, The evolution of insect metamorphosis: A developmental and endocrine view. *Philos. Trans. R. Soc. Lond. B Biol. Sci.* **374**, 20190070 (2019).
21. Y. Cui, Y. Sui, J. Xu, F. Zhu, S. R. Palli, Juvenile hormone regulates *Aedes aegypti* Krüppel homolog 1 through a conserved E box motif. *Insect Biochem. Mol. Biol.* **52**, 23–32 (2014).
22. M. Jindra, S. R. Palli, L. M. Riddiford, The juvenile hormone signaling pathway in insect development. *Annu. Rev. Entomol.* **58**, 181–204 (2013).
23. M. Broemer, P. Meier, Ubiquitin-mediated regulation of apoptosis. *Trends Cell Biol.* **19**, 130–140 (2009).
24. M. G. Guenther *et al.*, A core SMRT corepressor complex containing HDAC3 and TBL1, a WD40-repeat protein linked to deafness. *Genes Dev.* **14**, 1048–1057 (2000).
25. C. C. Tsai, H. Y. Kao, T. P. Yao, M. McKeown, R. M. Evans, SMRTER, a Drosophila nuclear receptor coregulator, reveals that EcR-mediated repression is critical for development. *Mol. Cell* **4**, 175–186 (1999).
26. C. Y. Lee *et al.*, E93 directs steroid-triggered programmed cell death in Drosophila. *Mol. Cell* **6**, 433–443 (2000).
27. S. Chafino *et al.*, Upregulation of E93 gene expression acts as the trigger for metamorphosis independently of the threshold size in the beetle *Tribolium castaneum*. *Cell Rep.* **27**, 1039–1049.e2 (2019).
28. S. George, S. R. Palli, Histone deacetylase 11 knockdown blocks larval development and metamorphosis in the red flour beetle, *Tribolium castaneum*. *Front. Genet.* **11**, 683 (2020).
29. G.-H. Zhu, Y. Jiao, S. C. R. R. Chereddy, M. Y. Noh, S. R. Palli, Knockout of juvenile hormone receptor, Methoprene-tolerant, induces black larval phenotype in the yellow fever mosquito, *Aedes aegypti*. *Proceedings of the National Academy of Sciences* 10.1073/pnas.1905729116 (2019).
30. T. Kayukawa, A. Jouraku, Y. Ito, T. Shinoda, Molecular mechanism underlying juvenile hormone-mediated repression of precocious larval-adult metamorphosis. *Proc. Natl. Acad. Sci. U.S.A.* **114**, 1057–1062 (2017).
31. T. T. Saha *et al.*, Synergistic action of the transcription factors Krüppel homolog 1 and Hairy in juvenile hormone/Methoprene-tolerant-mediated gene-repression in the mosquito *Aedes aegypti*. *PLoS Genet.* **15**, e1008443 (2019).

32. P. Karagianni, J. Wong, HDAC3: Taking the SMRT-N-CoRrect road to repression. *Oncogene* **26**, 5439–5449 (2007).
33. H. Oh, K. D. Irvine, Yorkie: The final destination of Hippo signaling. *Trends Cell Biol.* **20**, 410–417 (2010).
34. Y. Yin *et al.*, Histone deacetylase 3 overexpression in human cholangiocarcinoma and promotion of cell growth via apoptosis inhibition. *Cell Death Dis.* **8**, e2856 (2017).
35. Y. Kang, K. Marischuk, G. D. Castelvecchi, A. Bashirullah, HDAC inhibitors disrupt programmed resistance to apoptosis during *Drosophila* development. *G3 (Bethesda)* **7**, 1985–1993 (2017).
36. F. Escaffit *et al.*, Cleavage and cytoplasmic relocalization of histone deacetylase 3 are important for apoptosis progression. *Mol. Cell. Biol.* **27**, 554–567 (2007).
37. D. Denton, T. Xu, S. Dayan, S. Nicolson, S. Kumar, Dpp regulates autophagy-dependent midgut removal and signals to block ecdysone production. *Cell Death Differ.* **26**, 763–778 (2019).
38. Y. Wu, R. Parthasarathy, H. Bai, S. R. Palli, Mechanisms of midgut remodeling: Juvenile hormone analog methoprene blocks midgut metamorphosis by modulating ecdysone action. *Mech. Dev.* **123**, 530–547 (2006).
39. H. Chen, R. J. Lin, W. Xie, D. Wilpitz, R. M. Evans, Regulation of hormone-induced histone hyperacetylation and gene activation via acetylation of an acetylase. *Cell* **98**, 675–686 (1999).
40. Y. Kang, A. Bashirullah, A steroid-controlled global switch in sensitivity to apoptosis during Drosophila development. *Dev. Biol.* **386**, 34–41 (2014).
41. E. H. Baehrecke, Steroid regulation of programmed cell death during Drosophila development. *Cell Death Differ.* **7**, 1057–1062 (2000).
42. J. Doherty, E. H. Baehrecke, Life, death and autophagy. *Nat. Cell Biol.* **20**, 1110–1117 (2018).
43. A. J. Hörlein *et al.*, Ligand-independent repression by the thyroid hormone receptor mediated by a nuclear receptor co-repressor. *Nature* **377**, 397–404 (1995).
44. S. C. Gaddelapati, M. Kalsi, A. Roy, S. R. Palli, Cap 'n' collar C regulates genes responsible for imidacloprid resistance in the Colorado potato beetle, *Leptinotarsa decemlineata*. *Insect Biochem. Mol. Biol.* **99**, 54–62 (2018).
45. R. K. Dhandapani, D. Gurusamy, J. L. Howell, S. R. Palli, Development of CS-TPP-dsRNA nanoparticles to enhance RNAi efficiency in the yellow fever mosquito, *Aedes aegypti*. *Sci. Rep.* **9**, 8775 (2019).
46. W. S. Abbott, A Method of Computing the Effectiveness of an Insecticide. *J. Econ. Entomol.* **18**, 265–267 (1925).
47. K. J. Livak, T. D. Schmittgen, Analysis of relative gene expression data using real-time quantitative PCR and the 2(-Delta Delta C(T)) Method. *Methods* **25**, 402–408 (2001).
48. J. Ye *et al.*, WEGO: A web tool for plotting GO annotations. *Nucleic Acids Res.* **34**, W293–W297 (2006).
49. D. Bu *et al.*, KOBAS-i: Intelligent prioritization and exploratory visualization of biological functions for gene enrichment analysis. *Nucleic Acids Res.* **49** (W1), W317–W325 (2021).
50. B. T. Weinert *et al.*, Proteome-wide mapping of the Drosophila acetylome demonstrates a high degree of conservation of lysine acetylation. *Sci. Signal.* **4**, ra48 (2011).
51. M. H. Shihan, S. G. Novo, S. J. Le Marchand, Y. Wang, M. K. Duncan, A simple method for quantitating confocal fluorescent images. *Biochem. Biophys. Rep.* **25**, 100916 (2021).